



**GEOLOGICAL SURVEY OF CANADA**  
**OPEN FILE 3042**

---

Lithological and geophysical logs of shallow  
boreholes across the floodplain of the  
Red River, near St. Jean Baptiste, Manitoba

---

**G.R. Brooks, B.E. Medioli, J.A.M. Hunter, M. Nixon, R.L. Good**

**2001**



**Lithological and geophysical logs of shallow boreholes across the floodplain of the  
Red River, near St. Jean Baptiste, Manitoba**

G.R. Brooks, B.E. Medioli, J.A.M. Hunter, M. Nixon, and R.L. Good

Terrain Science Division  
Geological Survey of Canada  
601 Booth Street  
Ottawa, ON K1A 0E8

Geological Survey of Canada Open File Report 3042

5 February, 2001

## **Abstract**

Ten boreholes were cored into the alluvial floodplain of the Red River, Manitoba, in late September/early October 1999. The coring sites are located at two successive river meanders located about 2.5 and 3.5 km south-southeast (upstream) of St. Jean Baptiste. Detailed lithological logs depicting the detailed sedimentology of the boreholes reveal primarily silt alluvium overlying mud to clay glaciolacustrine deposits. These logs are supplemented by a diagram showing the height of the boreholes relative to the observed river surface, grain size diagrams, graphs depicting the vertical occurrence of  $\text{CaCO}_3$  precipitate and Fe-oxide mottling, and downhole geophysical logs showing measured natural gamma, electrical conductivity, magnetic susceptibility, relative density and gamma ratio.

## **Introduction**

The Red River, Manitoba, occupies a shallow stream-cut valley that is incised slightly into the flat clay plain of the Red River valley. The surface of this valley represents the genetic floodplain of the river and is the product of lateral migration of the river meanders (Brooks and Nielsen, 2000). The valley width is approximately equal to the amplitude of the meander belt, which is up to 2.5 km wide. During higher magnitude flows, the river discharge inundates the floodplain, overtops the sides of the shallow valley, and spreads laterally across the clay plain, forming a broad shallow flood zone within the Red River valley, as occurred in 1997, the largest Red River flood since 1852 (Rannie, 1998).

This Open File report contains lithological and downhole geophysical logs of ten boreholes cored into alluvium deposits of the stream-cut valley, near St. Jean Baptiste, Manitoba (Fig. 1). The purpose of the drilling program was to:

1. elucidate the evolution of the stream-cut valley and thereby determine whether valley-forming processes are compounding or diminishing the flood problem in the short-term, by significantly altering the cross-sectional area of the valley.
2. investigate the sedimentology of the floodplain. The Red River is a low-energy, suspended load river system and thus represents a river morphology that is poorly documented in the fluvial geomorphic literature.

The boreholes range in depth from 19.89 to 22.95 m and all are interpreted to have penetrated through alluvium into glacial Lake Agassiz lacustrine sediments. Chronological data and interpretations of the logs will be summarized in a subsequent report.

## **Location**

The coring sites are located on the alluvial floodplain at two successive river meanders located about 2.5 and 3.5 km south-southeast (upstream) of St. Jean Baptiste, Manitoba (Fig. 1). As depicted in Fig. 1, the boreholes are in two transects, consisting of five boreholes each, along the east and west sides of the valley bottom. The two transects are referred to as the 99RR1 and 99RR3 series with the individual boreholes designated with an A to E suffix (e.g., 99RR1A). The transects of boreholes extend from the proximal (A) to distal (E) floodplain (Fig. 1), and approximately follow the lateral migration of the channel, as revealed by a ridge and swale pattern on the floodplain that is visible on aerial photographs. All of the boreholes are located on cultivated fields.

## **Core collection**

The boreholes were drilled between September 27 and October 3, 1999, using a Mobile S-61 track-mounted drill rig and 7" hollow-stem auger (Fig. 2). The core was continuously sampled using a 3" (7.6 cm) OD (2.375" (6.0 cm) ID) split-spoon sampler that contained a clear acrylic tube liner. This liner received the core within the sampler

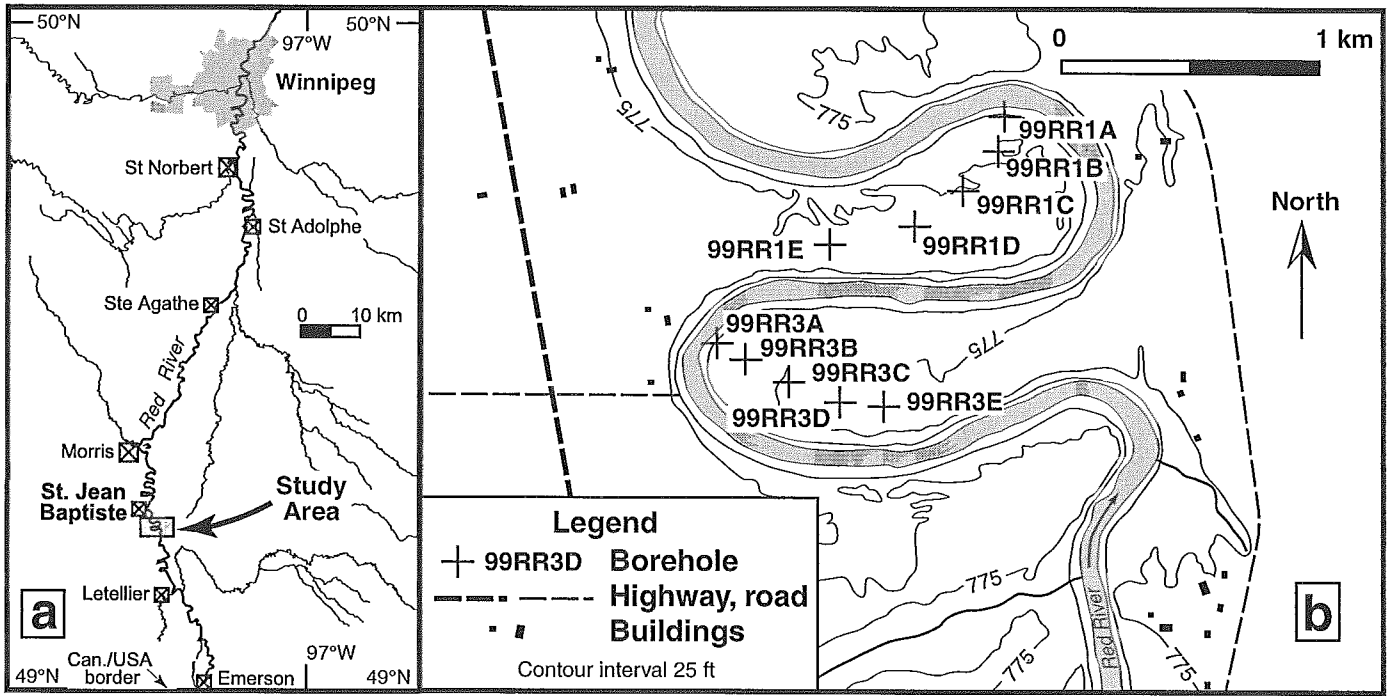


Fig. 1 Maps showing a) the general location of the coring sites in the Red River valley, Manitoba, and b) the locations of the ten boreholes across the river floodplain, near St. Jean Baptiste.



Fig. 2 Photograph of the Mobile S-61 track-mounted drill rig.

as the auger advanced into the ground, and then served as core container after recovery and splitting of the sampler. Drive depths were 20" (50.8 cm). Core recovery was excellent, but commonly exceeded 100% due to core expansion out of the ends of the sampler (Fig. 3, and see below). This expansion was confirmed against the drive depth of the auger, and almost certainly reflects the high proportion of clay and fine silt within the deposits and the saturated ground conditions below the water table (generally located at about 3.5 to 9 m depth). This 'excess' material was carefully collected, wrapped in aluminum foil and a plastic bag, and logged as part of the core sample, as described below.

Immediately upon removal from the split-spoon sampler, the sediment colour, texture and compaction of the core was described qualitatively from the ends of the core liner. The ends of each liner were covered with either a vinyl cap (depending on availability) or aluminum fold overlain with a small plastic bag, that were taped to form an air tight seal. The range of the auger drive depth was written on the liner, and the core was stored in wooden core boxes. The core boxes were subsequently shipped to GSC-Atlantic, Dartmouth, Nova Scotia, for detailed lithological logging and subsampling, as described below.

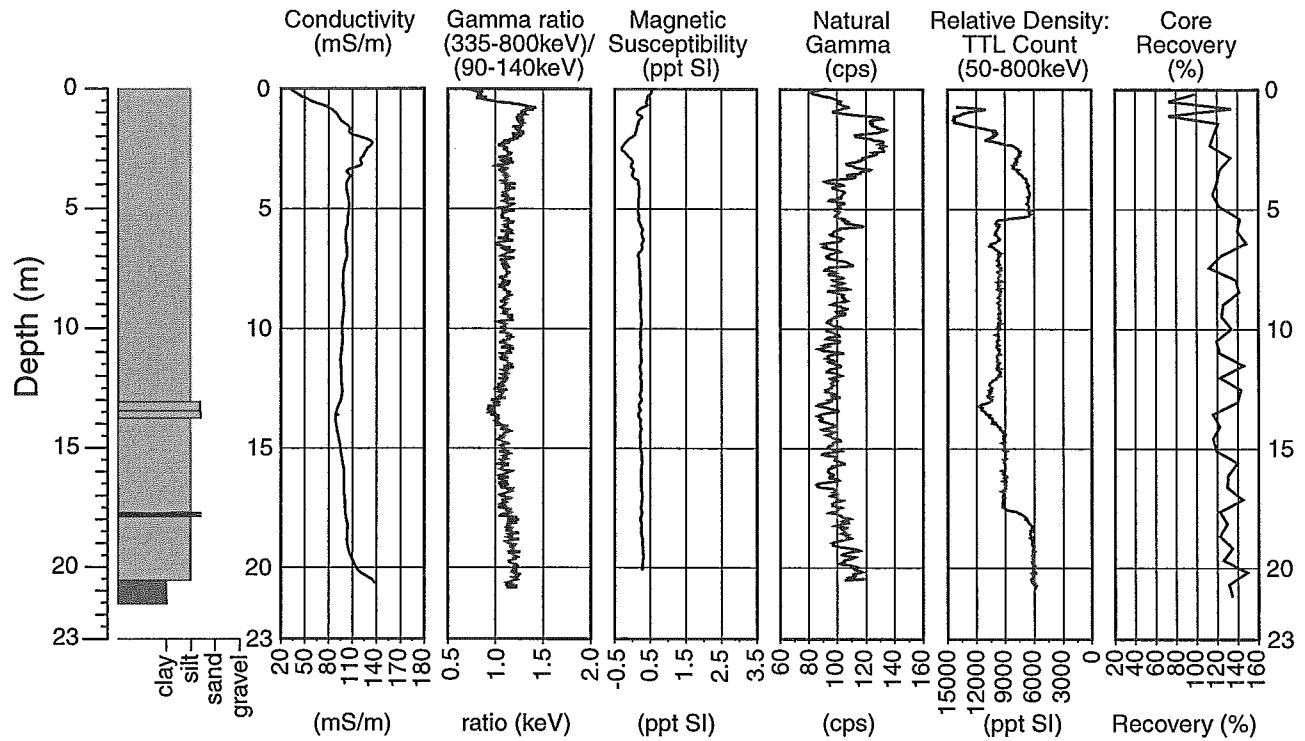
After completion of coring, the boreholes were cased with 3" (7.6 cm) PVC pipe; the top end of the casing was cut down to about 45 cm below the ground surface. The casing was capped and the annular gap grouted with bentonite. The borehole positions were fixed with differential GPS, and a piece of scrap steel was buried at each site immediately beside the top of the casing to facilitate locating the boreholes for future use. The geographical and UTM coordinates of the boreholes are listed in Table 1.

On October 29, 1999, the heights of the boreholes were surveyed relative to each other and the observed river water surface. The vertical heights of the boreholes along each series relative to the river surface are depicted in Fig. 4.

### **Lithological logs**

The lithology of the cores was logged in detail at the core logging facility, GSC-Atlantic, Dartmouth, Nova Scotia, between January 17 and 30, 2000. The cores were split, and logged to the mm scale for textural and structural sedimentology. The cores were subsampled for grain size analysis, macrofossils (wood, charcoal, shells), total organic carbon (TOC), and moisture content. For sediment analysis, bulk samples were collected over depths of 10 cm at about 2 m intervals as well as at some selected intervening depths. Unfortunately, the moisture content results are not reliable due to the loss of core sediment moisture in the period between core sampling and core logging, and thus are not reported. The general colour of the deposits was noted using a Munsell colour chart, and all of the cores were photographed, except between the depths of 2.55 to 3.06 m of borehole 99RR3B, which was inadvertently missed. Where there was core expansion (Fig. 3), the depth ranges of the core samples have been corrected relative to the drive depth of the augers.

### 99-Red River-1A



### 99-Red River-1B

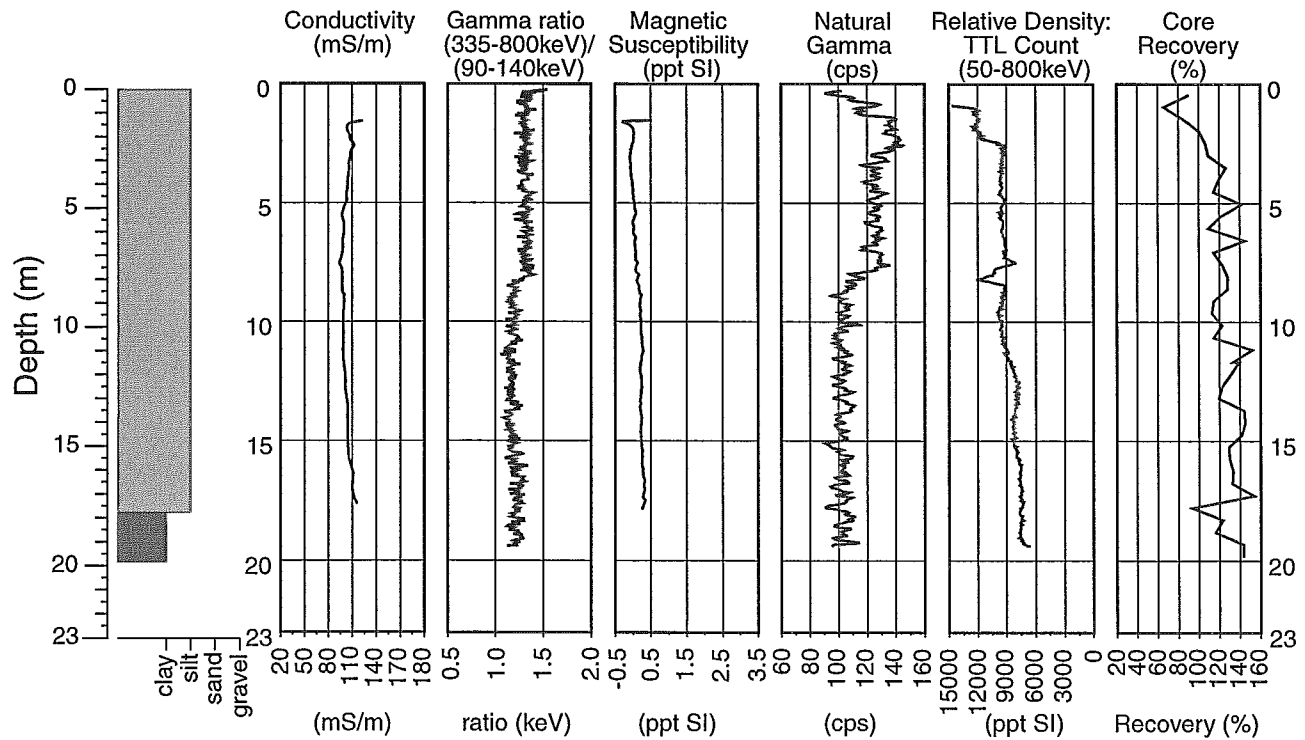
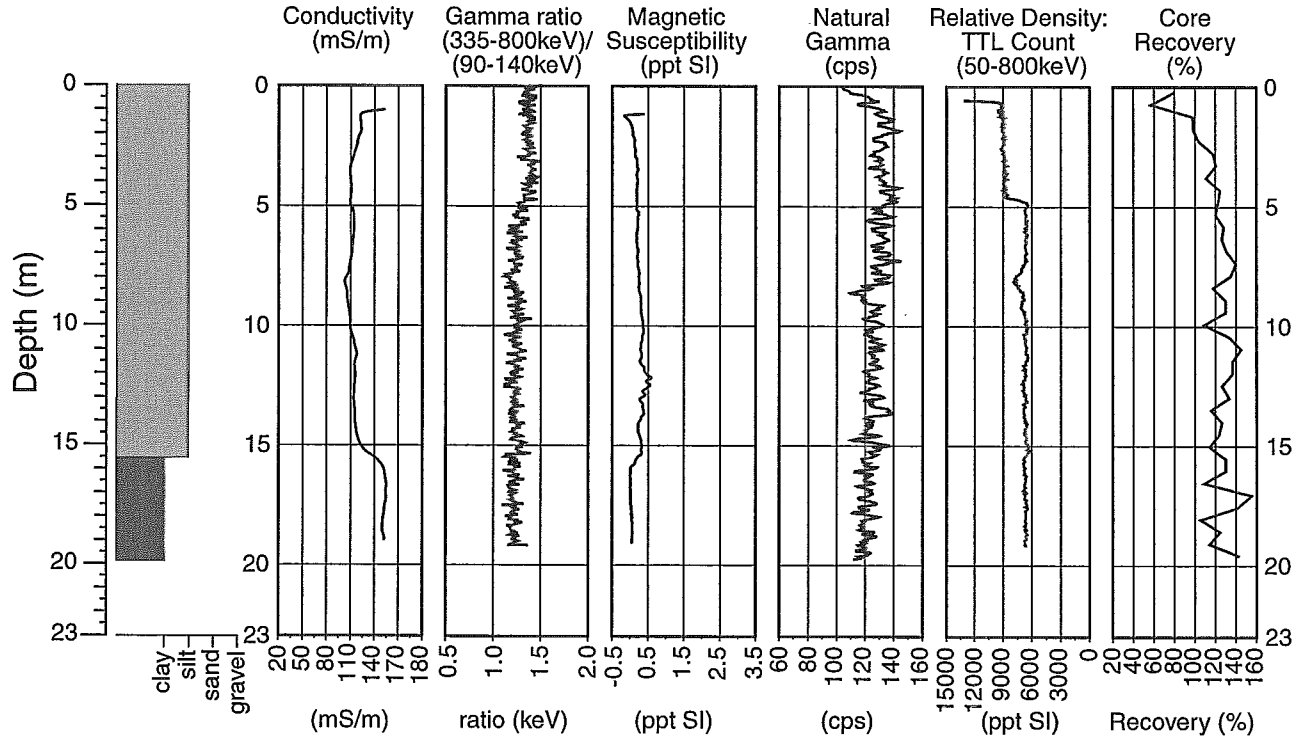
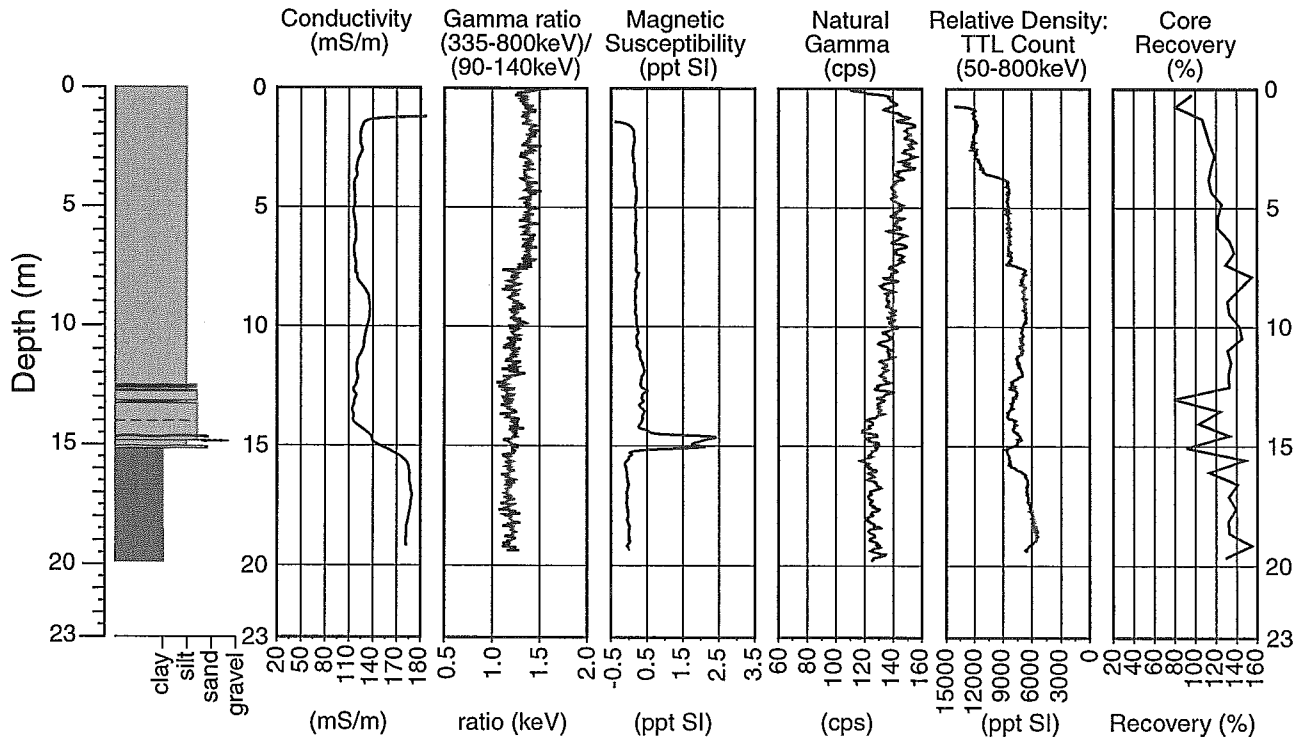


Fig. 3 Simplified borehole lithologies and the results of downhole geophysical logging, and percentage of core recovery for a) 99RR1A and 99RR1B, b) 99RR1C and 99RR1D, c) 99RR1E, d) 99RR3A and 99RR3B, e) 99RR3C and 99RR3D, and f) 99RR3E.

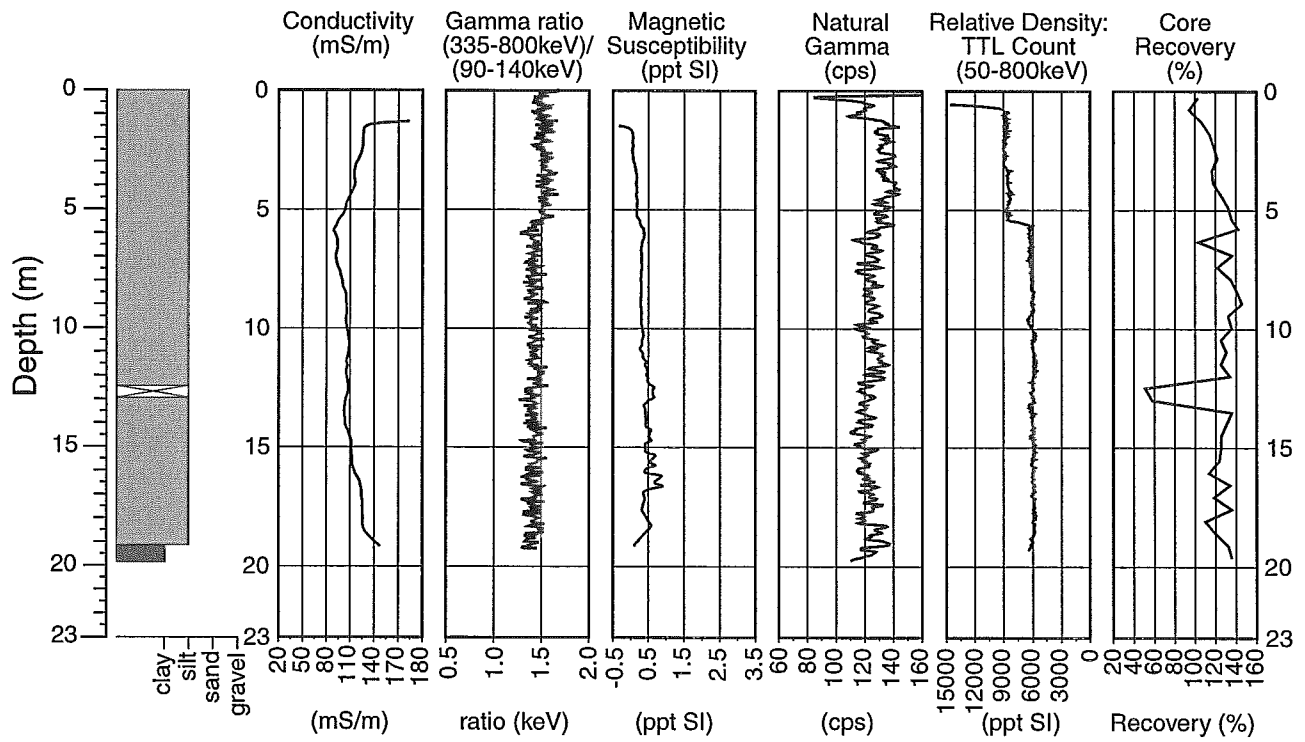
# 99-Red River-1C



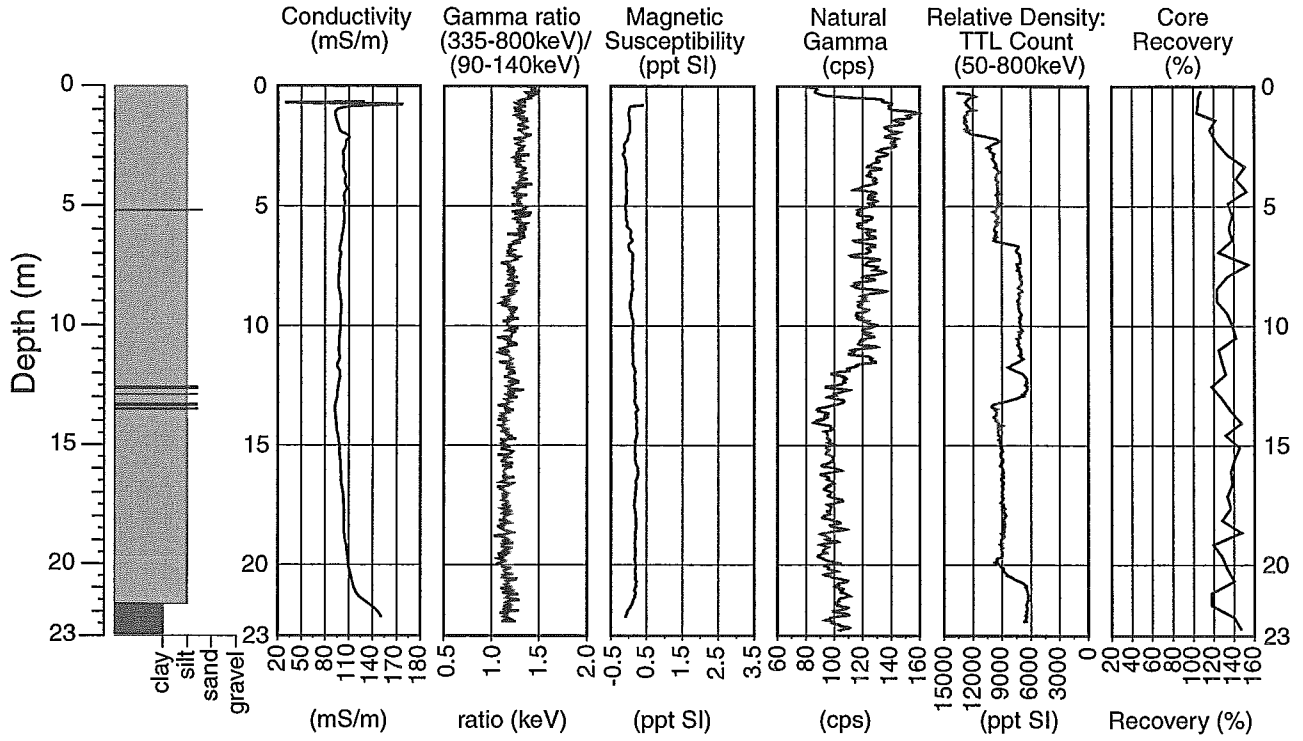
# 99-Red River-1D



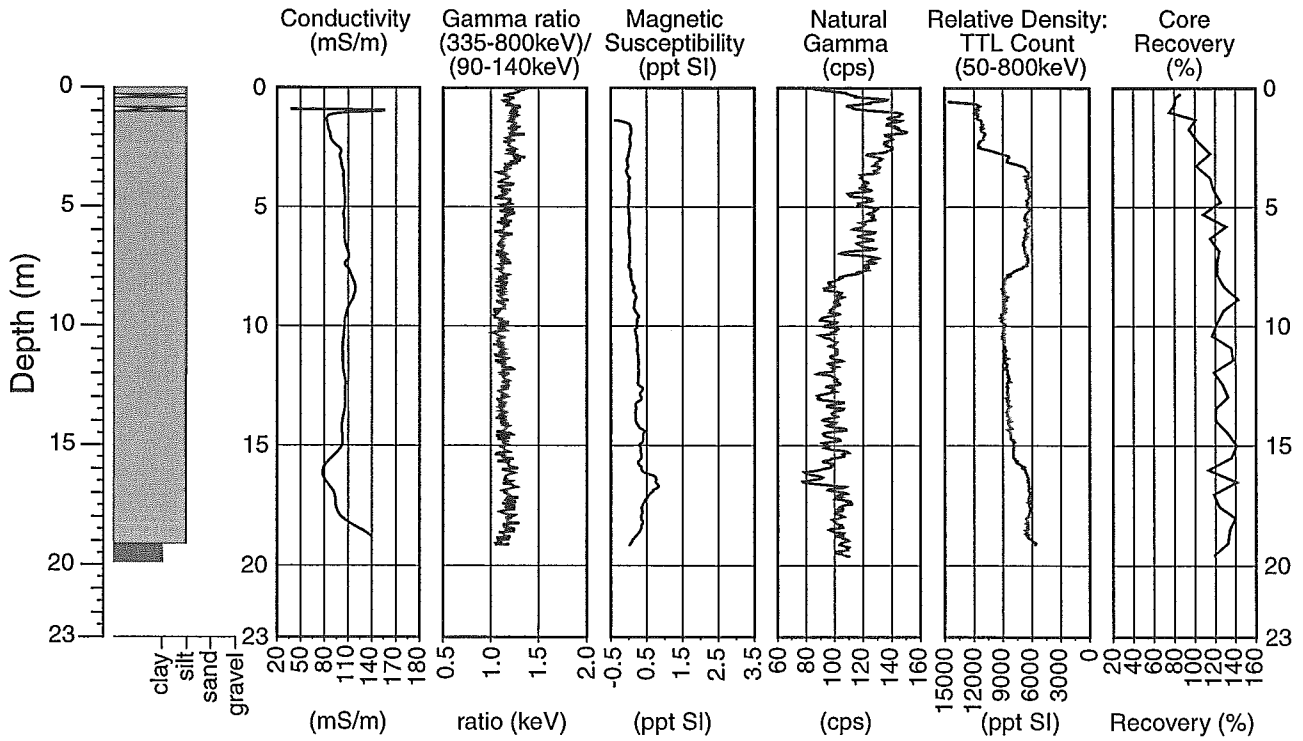
# 99-Red River-1E



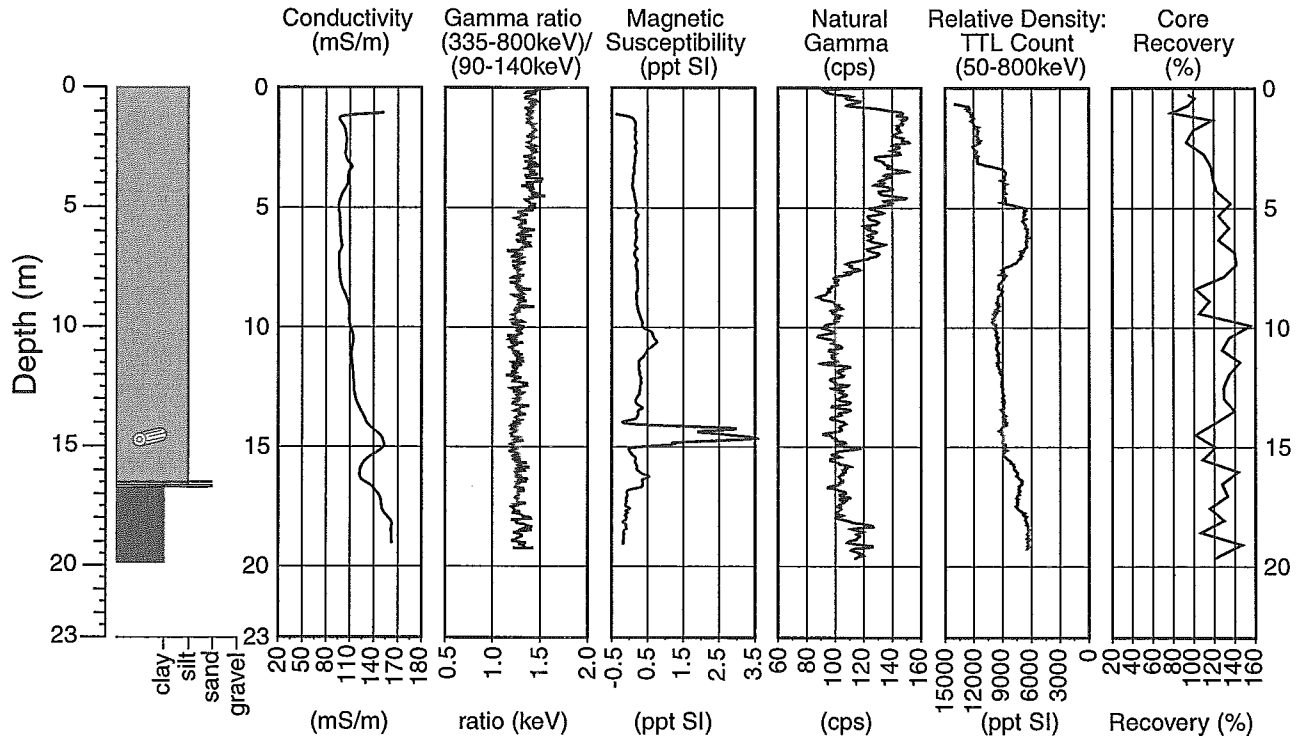
# 99-Red River-3A



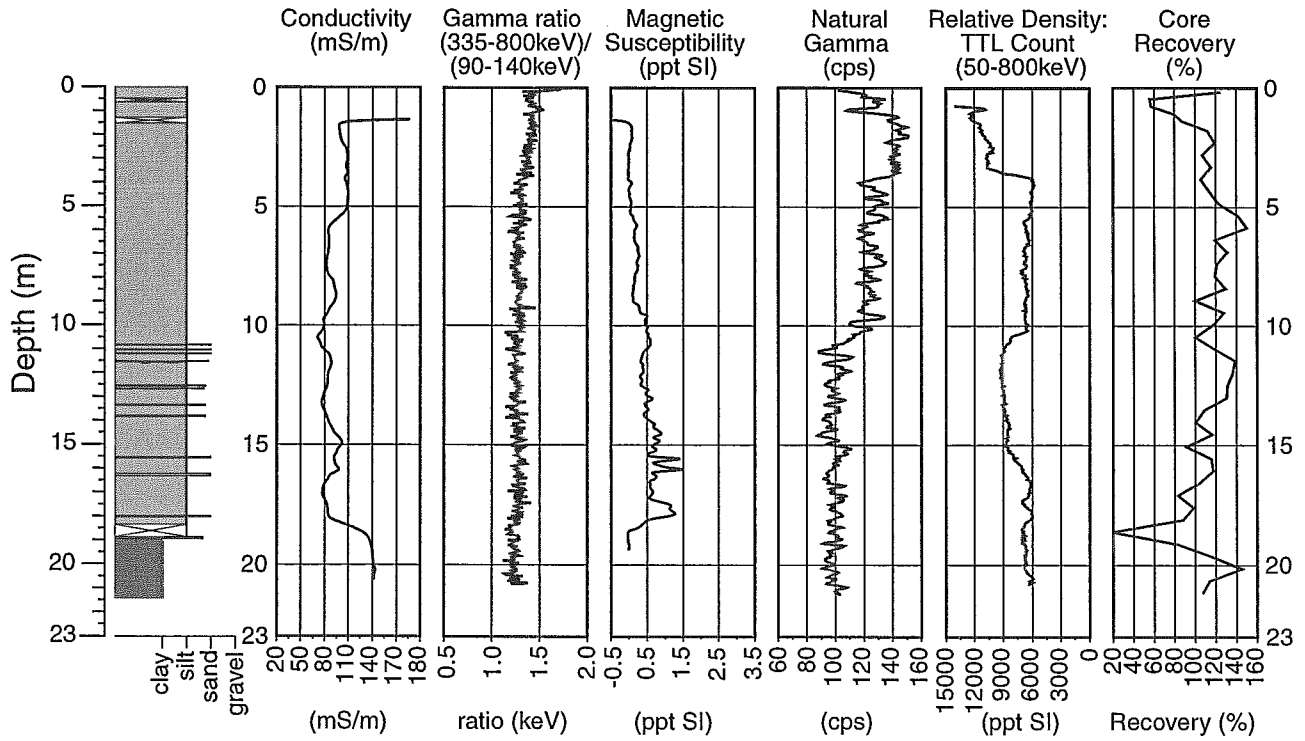
# 99-Red River-3B



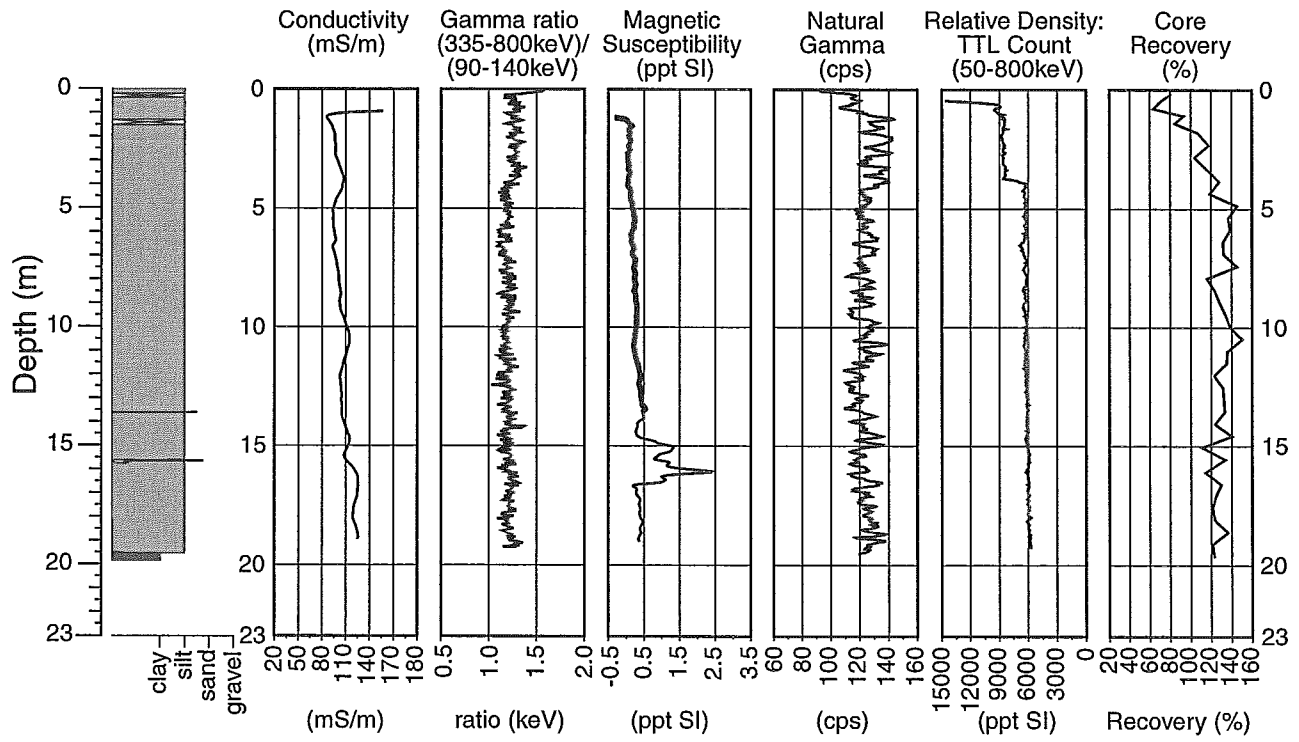
# 99-Red River-3C



# 99-Red River-3D



# 99-Red River-3E



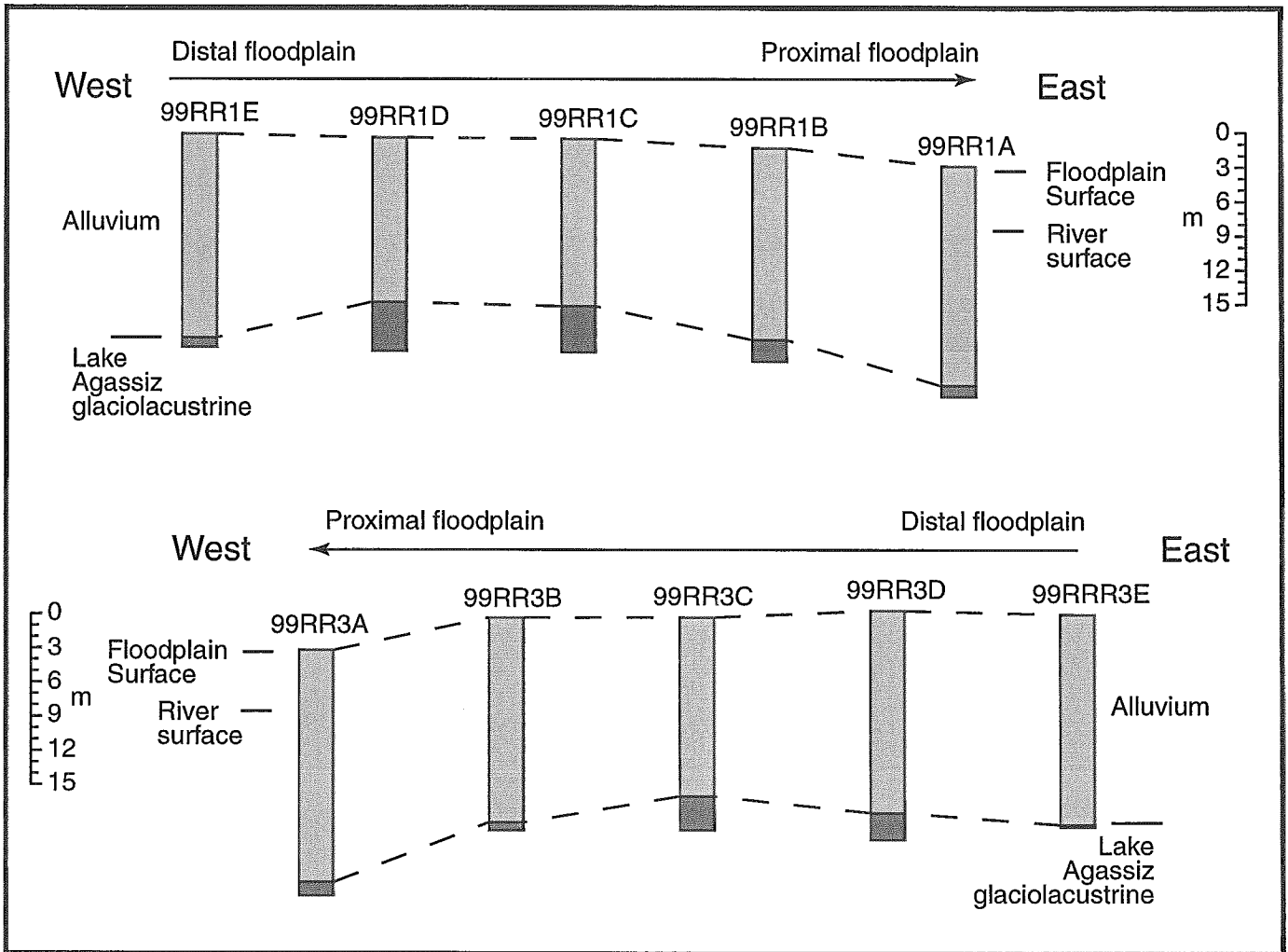


Fig. 4 Diagram showing the heights of the boreholes in each series relative to the river surface, and the general stratigraphy of the deposits. The boreholes in each series are arranged in sequence from the proximal to the distal floodplain.

Detailed lithological logs of the five boreholes in each series are depicted in Figs. 5 and 6 (pocket items). A wide variety of structural features of the deposits are represented symbolically on these logs. It should be noted that the sedimentology of the deposits is very subtle, reflecting the generally uniform fine-grained texture of the sediments. At first glance, the deposits commonly appeared massive when the cores were split, but careful examination revealed the subtle structures that were logged in detail. Also, at some depth ranges, post-depositional precipitate  $\text{CaCO}_3$  and Fe-oxide mottling, and disseminated organic matter, significantly masked the structure of the deposits. A pair of graphs that depict the vertical occurrence of the  $\text{CaCO}_3$  precipitate and Fe-oxide mottling accompany the lithological logs of each borehole. Definitions of the descriptor terms used on these graphs are listed in Table 2.

Sediment grain size analysis was undertaken at the Terrain Sciences Division Sedimentology Laboratory, using the techniques described by Klassen et al. (2000). A composite grain size diagram for the samples from each borehole is depicted in Fig. 7. The terms mud and clay used on Figs. 5 and 6 are based on the content of sand and the silt to clay ratio, following Folk (1965).

The general stratigraphy of the cores are shown on Fig. 4, and are defined as Red River alluvium and Lake Agassiz glaciolacustrine deposits. The unconformity between these two units is shown in each log on Figs. 5 and 6. This distinction is based on the presence of organic matter and a more complex sedimentology in the alluvial materials, and a markedly finer grain size distribution, the presence of  $\text{CaCO}_3$  precipitate, the occasional matrix-supported pebble (interpreted as a drop stone), and a characteristic massive structure in the glaciolacustrine deposits.

Core recovery expressed as a percentage of auger drive depth is depicted in Fig. 3. These percentages are based on the length of logged core rather than the field core logging notes, which are less accurate because of, for example, the presence of cuttings in the core liner. Some of the percentages may be moderately over or under exaggerated, depending on whether a portion of the 'excess' recovered core was inadvertently logged with the preceding or succeeding core. (The excess core from a single drive could be in two pieces: one from the bit at the base of the split spoon sampler, the other sticking out of the top of the sampler; each would be wrapped separately.) This occurrence does not change the fact that there was significant expansion of the core sediments.

### **Downhole geophysics**

Prior to the burial of the cased and grouted boreholes, downhole geophysics was undertaken using Geonics Ltd. EM-39 and IFG logging systems. Each borehole was logged for natural gamma, electrical conductivity, magnetic susceptibility, relative density and gamma ratio, and the results are presented in Fig. 3. The geophysical techniques and guides to interpretation of these logs are presented briefly below (also see Douma et al., 1999).

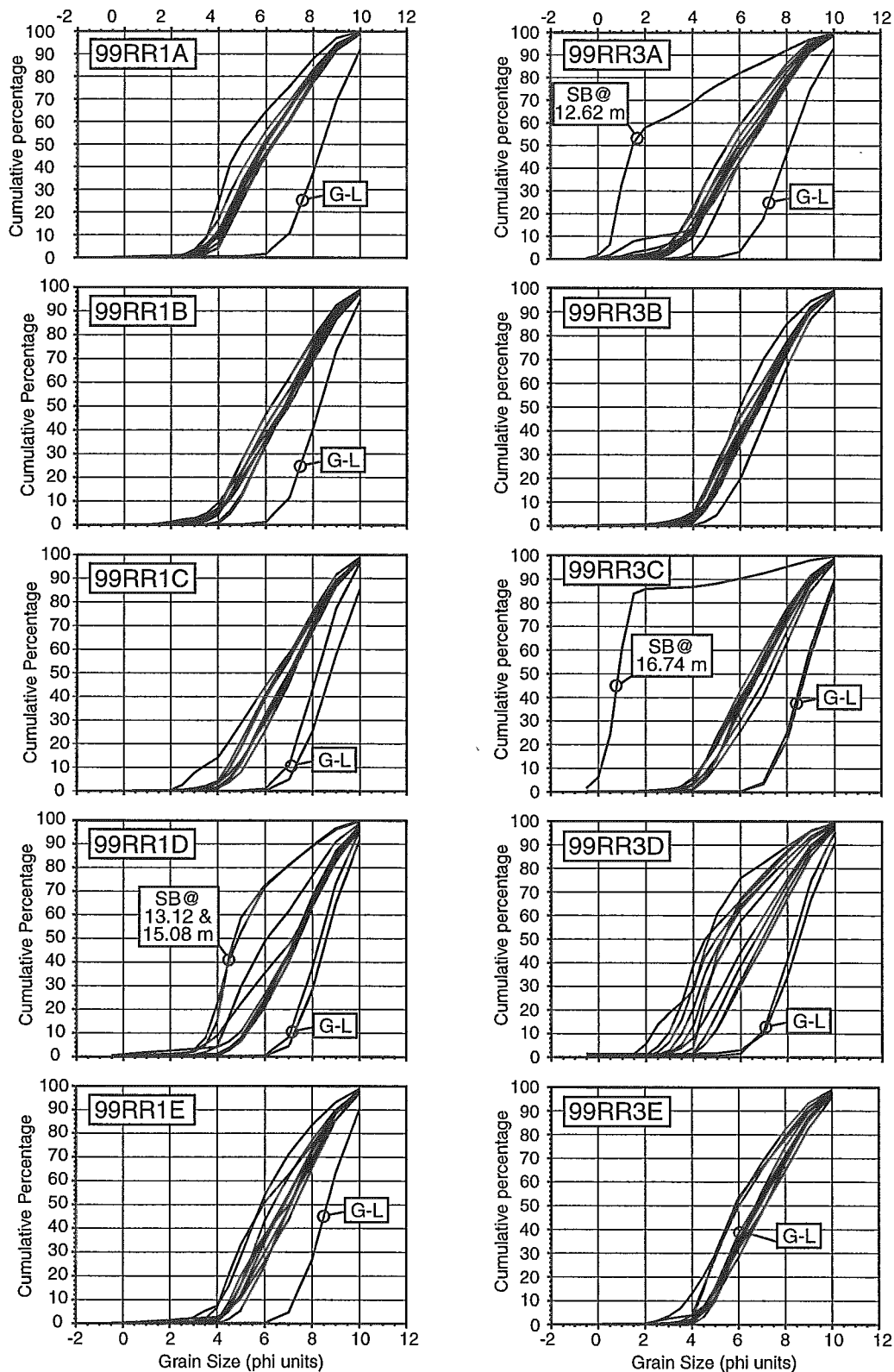


Fig. 7 Composite grain size diagrams for each of the 10 boreholes. Lake Agassiz glaciolacustrine sediments (G-L) are labeled for each core as are sand beds (SB), which are also flagged by sampling depth (e.g., @12.7 m). Lake Agassiz glaciolacustrine sediments were not sampled in core 99RR3B, but were in 99RR3E, even though there is no distinctively finer grain size curve for this sample.

### *Natural Gamma*

The down-hole natural gamma log was obtained using a Geonics Ltd. EM-39G logging system that uses a sodium iodide crystal to detect natural gamma radiation from in-situ sediments. Measurements were made at 2.5 cm intervals at a logging speed of 0.025 m s<sup>-1</sup>, allowing the use of high integration time (time constant of 5 seconds) and high precision counting statistics.

Radioactive isotopes of potassium, uranium and thorium occur naturally in unconsolidated sediments and the decay of these elements produces gamma rays. Changes in the measured count rate of gamma rays emitted from a formation can be used in a qualitative manner to estimate grain size, and to indicate lithological boundaries. In most sedimentary environments, high count rates are associated with fine-grained units (silts and clays), whereas low count rates are associated with coarser sediment (sand and gravel). For the borehole and casing diameters used in this survey, interpretative guidelines for estimating grain size are summarized in Table 3.

### *Electrical Conductivity*

The electrical conductivity log was obtained with the Geonics Ltd. EM-39C inductive electromagnetic sonde. This instrument contains 39 kHz tuned transmitter and receiver coils separated by 50 cm. The quadrature (out-of-phase) component of the received magnetic field is proportional to the average electrical conductivity of the ground between the coils. The unit has been specifically designed to be insensitive to near-hole effects such as borehole voids or saline drilling mud; however, the thickness of the formation contributing to the measured electrical field can exceed the intercoil spacing, resulting in a strong integration or smoothing effect (i.e. a sharp formation electrical contact will appear as a gradational change over a vertical distance of 50 cm or more). Prior to logging each borehole, a calibration of the probe was done to an accuracy of 0.1 mS/m. Logging speed was maintained at 0.030 m s<sup>-1</sup> to ensure digital sampling integrity.

The conductivity logs of these boreholes indicate relatively low values. Hence, the measured conductivities primarily reflect the conductivity of the sediment type rather than the electrical conductivity of the pore fluid. This log can be used in conjunction with the natural gamma log as a qualitative indicator of lithology. In general, coarse-grained sediments (sand and gravel) have relatively low conductivity values (~10-20 mS/m), whereas clay minerals usually are higher (~120-200 mS/m). Other factors affecting the measurements include moisture content and pore water salinity.

### *Magnetic Susceptibility*

The magnetic susceptibility log was obtained using the Geonics Ltd. EM-39M system. This tool is a two coil design similar to that of the inductive conductivity tool (EM-39C; described above). The measured in-phase magnetic field response of the instrument is a measure of the formation magnetic susceptibility and, hence, has a similar (but slightly less) depth of penetration and limitations in vertical resolution, as the induction

electromagnetic sonde. Prior to logging each hole, calibration of the tool was performed to an accuracy of 0.01 ppt SI. Logging speed was maintained at  $0.030 \text{ m s}^{-1}$ .

Magnetic susceptibility is a measure of the magnetization capacity of a material and is a dimensionless quantity (i.e., in effect the ratio of the induced to the applied magnetic field). In unconsolidated sediments, most of the response results from small quantities of magnetite. Hence, anomalously large values of bulk magnetic susceptibility in a formation are an indirect indication of increased heavy mineral content. There is, however, evidence of some exotic biogenic ferrimagnetic minerals giving rise to a significant magnetic susceptibility logging response, as has been found in glacial till deposits (P. Baumann, Komex Ltd., pers. comm., 2000).

### *Relative Density*

The IFG Ltd. gamma-gamma tool uses an uncollimated Cobalt-60 source and a  $25 \times 76$  mm Cesium Iodide crystal with a source-receiver spacing of 12.5 cm. Gamma ray energies from 0 to 3 MeV are measured over 256 evenly-divided energy channels. Relative density measurements are obtained from integrating the channels from 50 to 800 KeV, where most of the observed counts are to be found. The tool senses materials within a 30 cm radius of the sonde and the response is the combined effect of borehole fluid, casing, and the surrounding soil. The tool was operated at a logging speed of  $0.05 \text{ m s}^{-1}$  with samples at 1 second intervals.

Gamma ray interactions with soil include both photo-electric absorption at the low energy end of the spectrum, 0-180 keV, and Compton Scattering effects in the higher energy range from 180 keV out to the 3 MeV limit of the receiver. Soil density is inversely proportional to the observed gamma count rate due to Compton scattering. Since there is no calibration of density versus count rate available for densities in the range of typical soils and PVC cased boreholes, the data are plotted in Fig. 3 as counts per second. The results can be used in a qualitative manner only to infer variations in soil density. In holes where a well-defined groundwater table exists, this physical boundary is evident as a large deviation (towards high count rates) near the top of the logs.

### *Gamma Ratio*

This log is derived from the spectral information of the relative density log. The low energy end (<180 keV) of the observed gamma ray spectrum of earth materials obtained by using the gamma-gamma density sonde, is particularly sensitive to the average atomic number ( $Z$ ) of the formation (due to photoelectric absorption). Hence, by choosing a low energy and a high energy window, vertical changes in the count-rate ratio of these windows reflect changes in  $Z$ , but are insensitive to changes in formation density. In overburden materials, vertical changes in average  $Z$  might result from variation in heavy mineral content, void ratio, or moisture content. The spectral gamma-gamma ratios shown have low and high energy windows as indicated, and have been smoothed using a Svitsky-Golay smoothing function. A high value indicates high average atomic number  $Z$ .

## **Acknowledgements**

This work is part of a larger project undertaken by the Geological Survey of Canada and the Manitoba Geological Survey to investigate the paleoflood history of the Red River and geomorphic controls on the Red River flood problem. Funding for this work was provided by the Red River Flood Protection Program. We sincerely thank N. Beaudette, D. Manikel, and R. Sabourin for providing access to their properties, E. Nielsen and D. Berk (Manitoba Geological Survey) for logistical support, G. Matile (Manitoba Geological Survey) for the GPS measurements, S. St. George for assistance surveying, and I. Hardy for use of the core logging facilities at GSC-Atlantic. J. Guertin, T. Hunbert, and O. Lian assisted with the lithological core logging and subsampling. Drilling services were ably provided by Paddock Drilling Ltd., Brandon, Manitoba. Comments from S. Pullan on a draft of this report are appreciated.

## **References**

- Brooks G.R. and Nielsen, E.  
2000: Red River, Red River Valley, Manitoba; *The Canadian Geographer. Landscapes in Canada series*, v. 44, p. 304-309.
- Douma, M, Hunter J.A., and Good, R.L.  
1999: Borehole Geophysical Logging; *in A Handbook of Geophysical Techniques for Geomorphic and Environmental Research*, ed. R. Gilbert, Geological Survey of Canada Open File 3731, Chapter 4.
- Folk, R.L.  
1965: *Petrology of sedimentary rocks*; The University of Texas, Hempill's, Austin, 159 p.
- Klassen, R.A., Girard, I., Laframboise, R.R. and Lindsay, P.J.  
2000: A user's guide to the sedimentology laboratory, Terrain Sciences Division; Version 1.2.
- Rannie, W.F.  
1998: A survey of hydroclimate, flooding, and runoff in the Red River basin prior to 1870; Geological Survey of Canada Open File 3705, 189 p.

## Tables

Table 1 Boreholes locations

Borehole	Geographic Coordinates (latitude/longitude) <sup>1</sup>	UTM Coordinates (easting/northing) <sup>1,2</sup>	Horizontal Error at 2 $\sigma$ (m)
99RR1A	49.2465°N 97.3089°W	623080 5456234	0.7
99RR1B	49.2450°N 97.309720°W	623021 5456094	0.7
99RR1C	49.2439°N 97.3116°W	622885 5455937	0.7
99RR1D	49.2426°N 97.3142°W	622699 5455794	0.7
99RR1E	49.2420°N 97.3188°W	622370 5455716	0.7
99RR3A	49.2385°N 97.3241°W	621992 5455315	0.9
99RR3B	49.2379°N 97.3226°W	622104 5455254	0.8
99RR3C	49.2364°N 97.3203°W	622274 5455168	0.8
99RR3D	49.2364°N 97.3175°W	622476 5455095	0.7
99RR3E	49.2362°N 97.3152°W	622647 5455083	0.7

<sup>1</sup> WGS1984.

<sup>2</sup> UTM zone 14.

Table 2 Definitions of the proportions of CaCO<sub>3</sub> precipitate and Fe-oxide mottling on graphs in Figs. 5 and 6

Substance	Descriptor	Proportion of occurrence
CaCO <sub>3</sub> precipitate	Absent/trace	0-1%
	Light	1-5%
	Moderate	5-7%
	Heavy	7-15%
	Very Heavy	15-25%
Fe-oxide mottling	Absent/trace	0-1%
	Light	1-5%
	Moderate	5-7%
	Heavy	7-15%
	Very Heavy	15-25%

Table 3 Interpretative guides for natural gamma counts

Sediment texture	Gamma ray counts (cps)
Coarse sand/gravel	15-50
Dominantly fine sand	50-80
Dominantly silt	80-130
Clay	130-200